Appl. Phys. B 58, 51–56 (1994)

Applied Physics B Lasers and Optics

Preliminary Studies of Radiation Coupling Between Remote Soft X-Ray Laser Amplifiers

G. Cairns[1], C. L. S. Lewis[1], A. G. MacPhee[1], D. Neely[1], M. Holden[2], J. Krishnan[2], G. J. Tallents[2], M. H. Key[3,4], P. N. Norreys[3], C. G. Smith[4], J. Zhang[4], P. B. Holden[5], G. J. Pert[5], J. Plowes[5], S. A. Ramsden[5]

[1] Department of Pure and Applied Physics, Queen's University of Belfast, Belfast BT7 1NN, UK
[2] Department of Physics, University of Essex, Colchester CO4 2SQ, UK
[3] Central Laser Facility, Rutherford-Appleton Laboratory, Chilton, Oxon OX11 0QX, UK
[4] Clarendon Laboratory, University of Oxford, Oxford OX1 3PU, UK
[5] Department of Computational Physics, University of York, York YO1 5DD, UK

Received 12 July 1993/Accepted 4 October 1993

Abstract. Coupling of a soft X-ray laser beam with a relaying concave mirror in a sequentially pumped amplifier geometry using the Ne-like Ge system has been studied experimentally. Preliminary observations indicate an increase in the spatial coherence of the amplified relayed beam. In addition, near-field imaging of one of the amplifier plasmas shows a double-lobed intensity pattern of the emergent beam indicating refractive guiding of the amplified beam with components both normal and tangential to the target surface.

PACS: 42.60.By, 42.60.Kg, 42.10.Mg

We report an experiment carried out using the VULCAN glass laser facility at the Rutherford-Appleton Laboratory which marks the beginnings of a new era in the manipulation of X-ray laser beams and the development of cascaded amplifier technology. We have successfully coupled the 23.2 nm and 23.6 nm wavelength ASE outputs from a double-slab neon-like Ge amplifier into a second double-slab amplifier which is pumped almost 5 ns later. Coupling between the amplifiers is achieved in an essentially image-relayed mode using a concave X-ray mirror of focal length 25 cm and the experimental geometry is illustrated in Fig. 1. Components of this setup have been studied separately and previously reported, as discussed in the next section.

Our near-term objective is to generate saturated and spatially coherent output beams at wavelengths in the 15–25 nm range and this experiment, although a preliminary first attempt, has been encouraging. A similar geometry using a flat X-ray mirror and single foil targets of Ne-like yttrium has also been reported recently but with no initial claims for enhanced spatial coherence in the coupled beam [1].

1 Experimental Arrangement

A schematic of the slab target positions and their optical pump beams is shown in Fig. 2. Six VULCAN laser beams of 110 mm diameter and 1.05 μm wavelength were used in a standard off-axis illumination geometry to drive a double slab target consisting of two 18 mm long stripes (i.e. (18 + 18) mm) coated on glass substrates [2–5]. A Gaussian shaped pulse of duration 1.1 ns FWHM was used to drive 160 μm wide targets at an average irradiance of 1×10^{13} W cm^{-2}. The North propagating soft X-ray laser beam from this double target which will be referred to as the "injector" (see Fig. 1) was image-relayed and injected into an amplifier target situated in a newly commissioned second target chamber. Two 150 mm diameter beams were used in the second chamber in a staggered mode from opposite sides to drive (14 + 14) mm, 160 μm wide double slab targets also at an average irradiance of 1×10^{13} W cm^{-2}. These beams can be focused to a variable length line focus using a combination of two rotatable plano-concave cylindrical lenses of approximate focal length −3 m and a main aspheric focussing lens of focal length ≈40 cm. The X-ray mirror imaged the injector exit plane with a magnification of ≈3.3× to a plane ≈60 mm in front of the amplifier and the amplifier was optically pumped ≈4.8 ns later than the injector to allow for the transit time delay of the X-ray laser beam. Plasma uniformity along the axial direction of both the injector and amplifier plasmas was monitored using space resolving crystal spectrometers observing the resonance line emission in the 8–10 Å region. A streaked crystal spectrometer was also used to monitor the time varying emission from Ne- and F-like lines under different drive and target conditions.

Soft X-ray lasing signal levels from the injector and amplifier targets when they were pumped separately and operated without any coupling were initially monitored using a flat-field spectrometer to verify expected operation conditions in the component amplifiers. Initial evidence for coupling was observed with the same spectrometer but with only 1-D angular information available on a narrow slice of the output beam interpretation was sometimes difficult. 2-D information was obtained by using a second X-ray mirror to preferentially reflect the 23.2 nm and 23.6 nm radiation from the plasma amplifiers onto a camera back to record a "footprint" of the beam. Kodak 10402 film was used and baffled from plasma light with an 0.8 μm thick aluminium

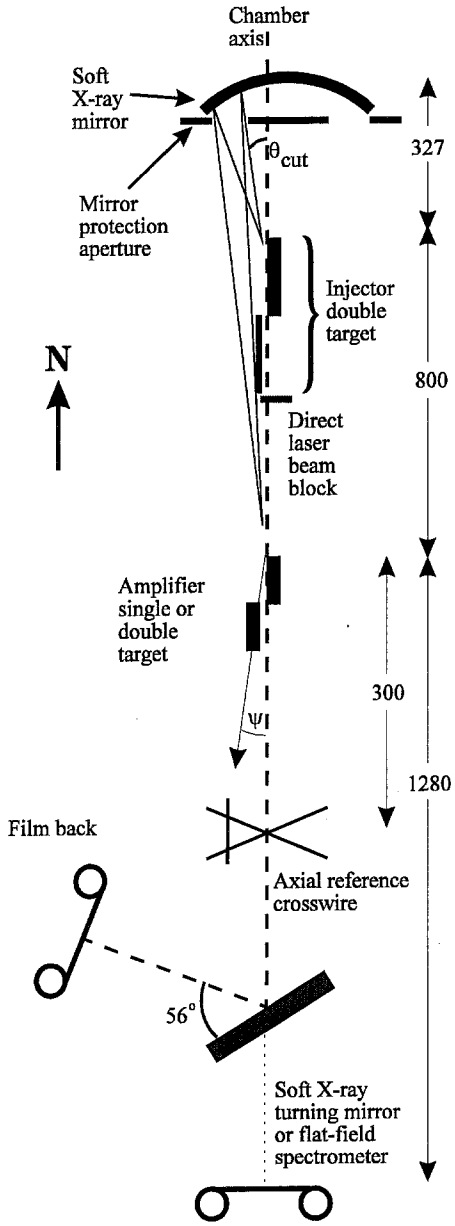

Fig. 1. Schematic of coupling arrangement between a double slab injector and a double slab final amplifier using a concave X-ray mirror. The layout of the beam "footprint" monitor is also shown. Marked dimensions are in mm

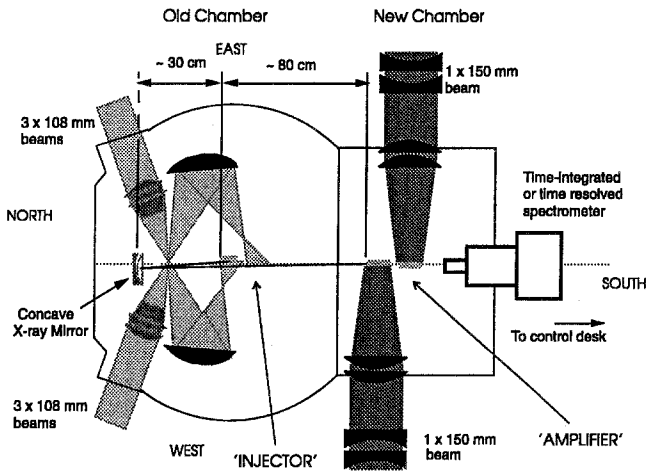

Fig. 2. Schematic showing the overall experimental layout including the optical pump beam lines and focussing optics

filter. The second mirror was planar and used at an incidence angle of 34 degrees for maximum effect at 23.4 nm and the total path length from the final amplifier to film was ≈1.3 m. Various reference wires were used in the X-ray mirror alignment system and it is from an analysis of the Fresnel fringe patterns generated from these wires and observed in the beam footprints that we infer changes in the spatial coherence of the beam. A more rigorous diagnostic based on interference from a Young's slits structure combined with a diffracting element giving wavelength isolation of the different laser lines was also used in this experiment and data from this diagnostic will be presented in a separate publication [6].

2 Beam Injection into Slab Amplifiers

In this experiment we had a relatively low pump irradiance and hence low gain-length products were achieved. Since stripe widths were also rather wide the net effect was a beam emanating from the injector double target with poor divergence. This was measured, as discussed in the Sect. 4 below, and at FWHM was typically 25 mrad and 10 mrad in the planes parallel and perpendicular to the target surfaces, respectively. Such a beam (at 23.2 nm and 23.6 nm wavelengths) after reflection by the X-ray mirror effectively had a divergence of ≈8 mrad and ≈3 mrad in the vertical and horizontal planes when injected into the final amplifier stage. Assuming shot-to-shot reproducibility we have attempted to monitor the effect of the final amplifier as the separation between the surface planes of the two 14 mm slab components was varied. This is illustrated in Fig. 3 where the footprints have all been recorded at ≈1.3 m from the final amplifier. In this sequence of five shots the separation between double slab surfaces varies from 300 μm to 150 μm (Fig. 3b–e) and in one case there is only a single slab amplifier (Fig. 3a). Clearly the pointing direction of the exiting beam is being controlled by refraction effects in the plasma zones within which the propagating beam is able to transit. The integrated output beam energy is also determined by the relative positions of the two slab amplifiers and the enhancement due to the second slab can be gauged by comparing the total energy output to the single slab only case. For the present conditions the peak energy enhancement obtained in using the second slab is ≈12×, corresponding to Fig. 3a, d. Another interesting feature of the images displayed in Fig. 3 is the wispy-like or striated intensity structures present. We believe that these are associated with inhomogeneities in the gain region and our intentions are to study these features in more detail in a future experiment.

More interestingly, we see that in the single target amplifier the final beam divergence in the vertical direction has been reduced from a nominal input value of ≈8 mrad to ≈2.7 mrad in this case. This is shown in more detail in Fig. 4.

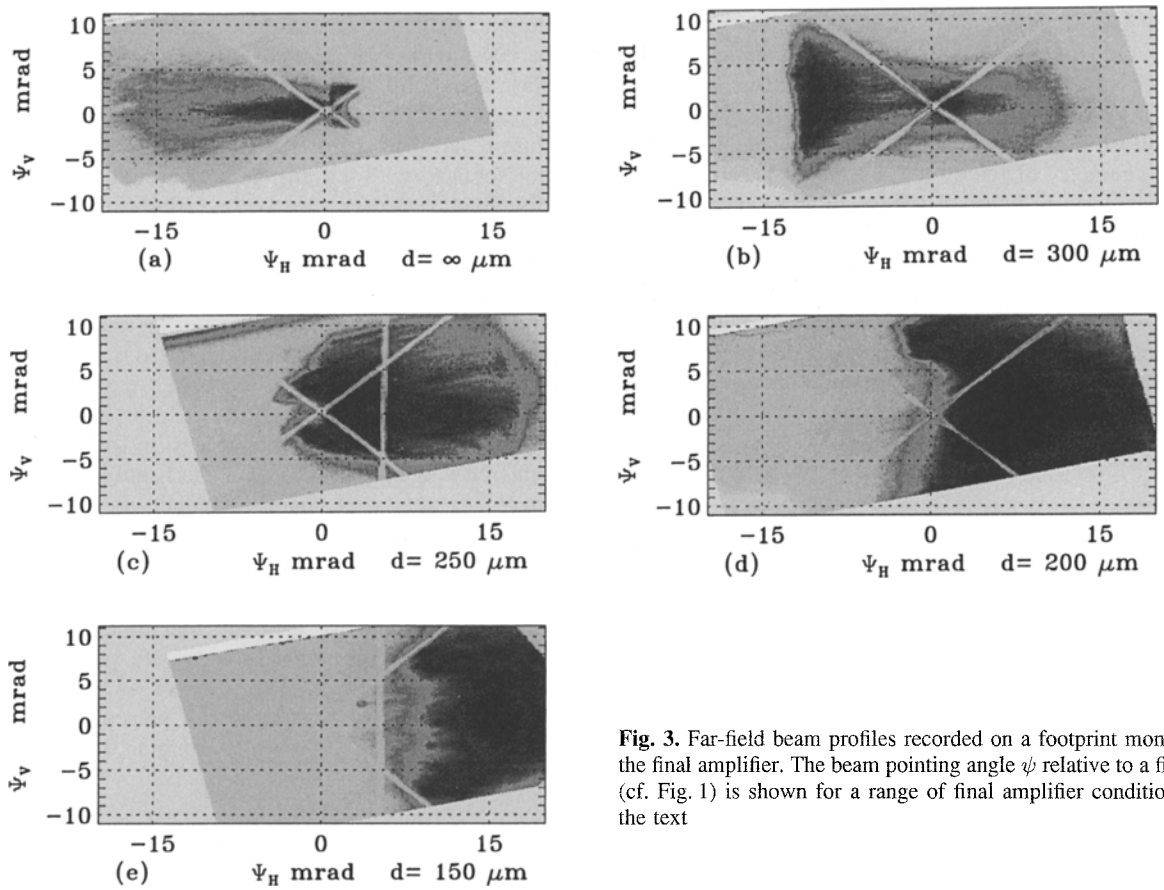

Fig. 3. Far-field beam profiles recorded on a footprint monitor at ≈1.3 m from the final amplifier. The beam pointing angle ψ relative to a fixed axial cross-wire (cf. Fig. 1) is shown for a range of final amplifier conditions, as discussed in the text

However, the horizontal divergence has increased from a nominal value of ≈3 mrad to ≈11 mrad and is dominated by refractive spreading of the beam's angular distribution. Nevertheless, in the vertical direction this very narrow angular distribution of a bright beam is indicative of a high degree of spatial coherence in this direction. This effect was observed on several shots but on other apparently identical shots the divergence observed was significantly worse, indicating sensitivity to actual plasma conditions. In the case of double slab amplifiers we observe that in all shots taken the beam divergence increases significantly in both planes so that the observed beam brightness enhancement factor over the single slab case is only ≈2–3×. It is clearly imperative to find ways to minimise the destructive refractory effects in these amplifiers.

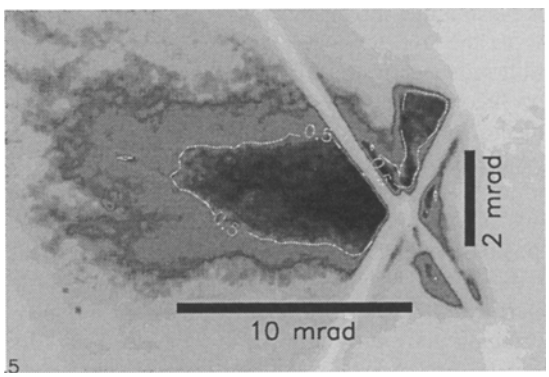

Fig. 4. Enlarged image of Fig. 3a showing clearly the very narrow beam divergence obtained in the plane parallel to a final amplifier slab. The contour shown is at the half peak intensity level

The injector beam was focussed to a plane in front of the final amplifiers. The beam incident on the final amplifiers was therefore divergent and overfilled the plasma region. When coupling into single target amplifiers we routinely obtained quasi-point projection shadowgraphs of the amplifier plasma radial structure which show up as an absorption region in the footprint of the beam which is undeflected by the amplifier. An example is seen in Fig. 3a where the footprint on the right-hand side of the cross-wire reference (i.e. $\psi > 0$) represents the undeflected incident beam and the footprint on the left-hand (i.e. $\psi < 0$) represents the part of the incident beam which has been coupled, amplified and deflected through refraction effects. The plasma shadow is the half moon segment missing on the right of the image and the slab target surface corresponds to a vertical line at the extreme right of the image. In this particular case the clarity of the effect is compromised slightly by the presence of the reference cross-wires. The undeflected beam on this shot has a rectangular appearance because of several restricting apertures defined by the target surfaces and field stops at the mirror plane. Although we would expect the plasma cross-sectional area observed in the shadow to be larger than the gain region cross-sectional area we can attempt to compare the missing energy in the undeflected beam to the total energy in the deflected beam to

estimate the energy gain achieved in the amplifier. This was done by digitising and integrating over the relevant image areas and using the film calibration curves. Typically 2–3% of the relayed injector beam energy was observed to be missing in the shadow region and this is roughly what is expected from the geometry of the system assuming a gain zone in the plasma of scale-length ≈100 μm. For a single 14 mm target final amplifier the observed energy ratio was between ≈20–70×. Assuming that the output energy is given by the input energy times the exponential of the gain length product of the spectral lines of interest then this corresponds to a gain coefficient of $2.5 \pm 0.5\,\mathrm{cm}^{-1}$ which is consistent with our earlier measurements of gain coefficients at these intensities [3].

3 Spatial Coherence

One of our primary aims during this experiment was to increase the spatial coherence of the output laser beam. A rough estimate of the benefits of injecting the beam into single and double slab target amplifiers can be obtained from a measurement of the central Fresnel fringe visibility in the geometrical shadow region of the axial reference cross-wires. An intensity distribution obtained from one of the 180 μm cross-wires which were situated at ≈300 mm from the plasma and at 920 nm from the film pack is shown in Fig. 5. A number of shots were analysed and the observed fringe visibilities are shown in Fig. 6. The large error bars present are associated with the difficulty in accurately measuring the fog level. However, clearly the visibility increases as additional amplifier targets are inserted, which suggests that the spatial coherence is improving. These observations are complementary to the Young's slits measurements also made [6] and both sets of data are being further analysed to quantify the degree of spatial coherence achieved. An interesting observation was that on a few shots the fringe visibility varied considerably depending on the position along the wire sampled. This would suggest that at least in some cases the beam coherence is not uniform over the beam profile.

Preliminary attempts were made to reduce the number of modes being injected into the amplifier by reducing the aperture of the relay mirror. Coherence measurements from this parameter scan are presently being analysed. However, from earlier measurements we estimate that to illuminate the amplifier with a coherent wave front would require an aperture of ≈200 μm diameter. This is over an order of magnitude smaller than was tested in the present run as detectability was limited by the low gain-lengths achieved.

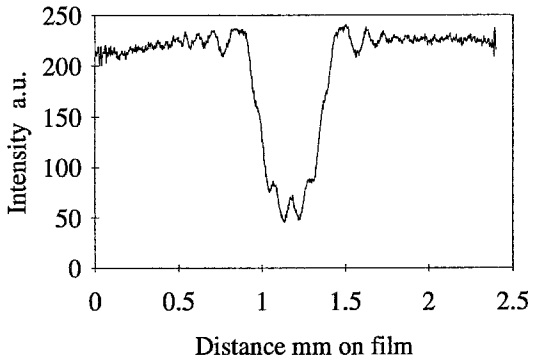

Fig. 5. A typical line-out of the Fresnel fringe intensity pattern recorded from a 180 μm diameter wire in the soft X-ray layer beam

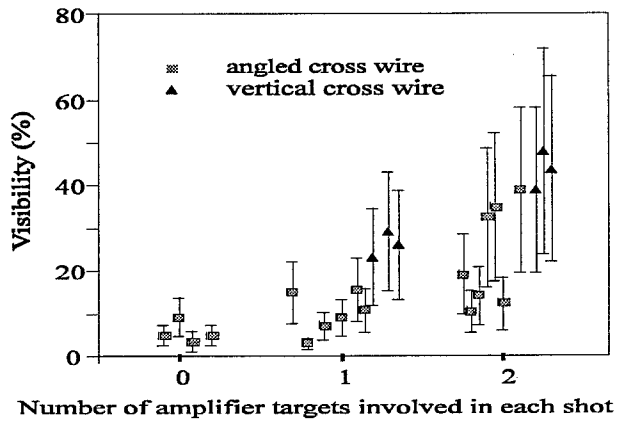

Fig. 6. The fringe visibility is seen to increase with the gain-length product of the system implying increasing spatial coherence in the relayed and amplified beam

4 Near- and Far-Field Beam Distributions

All of our earlier studies of the soft X-ray laser beam cross section have only been possible in the far field due to diagnostic limitations [2–5]. Although this can give us accurate information on the beam divergence it provides little information on the uniformity, size and distribution of the beam as it exits the plasma. Such near-field information is useful for additional comparison with code predictions and was obtained here by imaging. This was done by leaving the footprint monitor in its position as described above and moving the relay X-ray mirror to image planes at different distances from the injector exit plane onto film. The final amplifiers discussed above were absent for these shots. Typically the magnification was ≈8.5× and near-field images corresponding to distances 0, 18, and 48 mm from the injector plasma are shown in Figs. 7b–d. Figure 7a also corresponds to the injector exit plane but in this case for a stripe width reduced from 160 μm to 115 μm. A far field beam pattern recorded on a footprint monitor placed ≈1.2 m from the injector plasma is shown in Fig. 7e.

A noticeable feature of this sequence is the double-lobed structure observed in the beam profile close to the injector. This is shown in more detail in Fig. 8 where the estimated position of the target stripe is also shown. This structure is due to refractive effects in the plane parallel to the target surface which will have an up-down symmetry. A 3-D ray tracing code presently being developed at York University gives good qualitative agreement with these near-field observations and a wave code also under development will be able to model the beam evolution from near- to far-field [7].

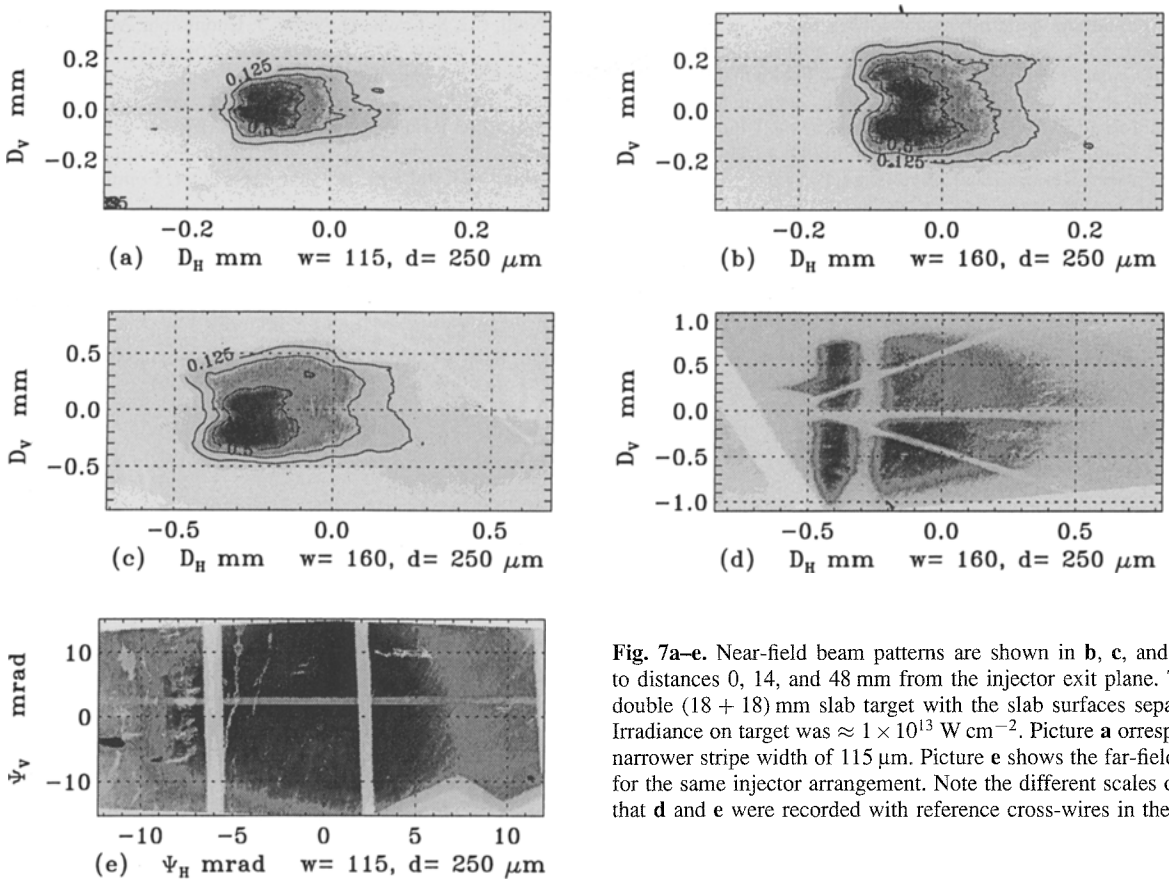

Fig. 7a–e. Near-field beam patterns are shown in **b**, **c**, and **d** corresponding to distances 0, 14, and 48 mm from the injector exit plane. The injector was a double (18 + 18) mm slab target with the slab surfaces separated by 250 μm. Irradiance on target was $\approx 1 \times 10^{13}$ W cm^{-2}. Picture **a** orresponds to **b** but for a narrower stripe width of 115 μm. Picture **e** shows the far-field pattern at ≈1.2 m for the same injector arrangement. Note the different scales on each picture and that **d** and **e** were recorded with reference cross-wires in the beampath

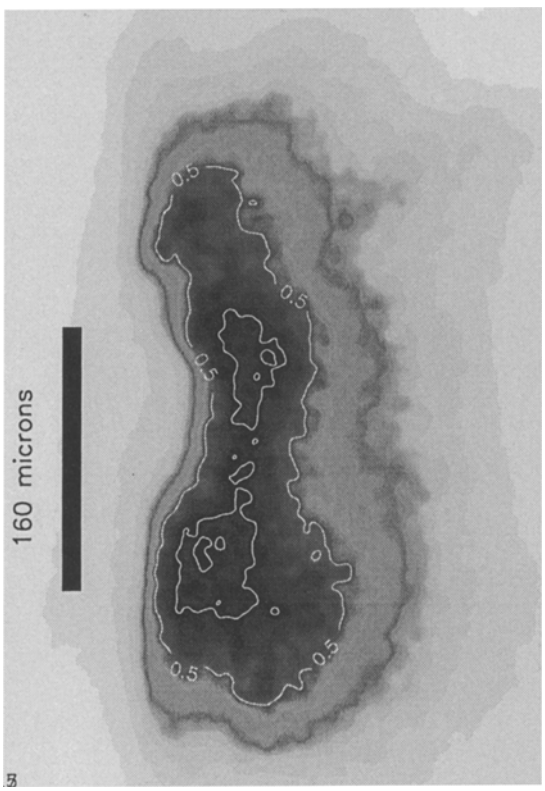

Fig. 8. Enlarged image of Fig. 7b clearly showing the double-lobed near-field structure. The position of the target (drawn to scale in the vertical direction) is estimated from earlier work and is consistent with modelling. The contours are at 0.5 and 0.7 peak intensity levels

5 Concluding Remarks

We have successfully demonstrated coupling using a relaying concave soft X-ray mirror in a sequentially pumped amplifier geometry. This mirror was situated sufficiently far away from the plasma (≈30 cm) that multiple use of the same surface elements did not appear to significantly degrade mirror performance. However the effective multi-shot reflectivity for the mirrors used did not exceed ≈5% and there is some indication that the mirror performance may have been closer to the expected reflectivity value of ≈20% on the first exposure to plasma light. Preliminary results indicate that the spatial coherence in the output beam from a double amplifier was significantly higher than in the injected beam. Near-field images showing features reminiscent of two lobes from 160 μm wide double targets have been observed. This indicates a horizontal plane of symmetry within the gain zone with refracting beamlets propagating outwards on either side of it. This is in addition to an overall refraction effect sending both beamlets away from the vertical plane containing the target surface.

We plan to demonstrate in the near future that by using a higher reflectivity and apertured X-ray mirror combined with optimised and higher gl (gain-length product) amplifier designs that it will be possible to achieve a fully coherent and saturated output beam.

Acknowledgements. The authors gratefully acknowledge the technical and operational support given by all the staff of the central Laser Facility at Rutherford-Appleton Laboratoy. We would also like to thank Mr. W. J. Conn of Queen's University, Belfast, for his help in the preparation of target substrates. This work was supported by the United Kingdom Science and Engineering Research Council through a rolling grant entitled "X-ray Lasers: Research and Development".

References

1. G.N. Shimaveg, M.R. Carter, R.S. Walling, J.M. Ticehurst, R.A. London, R.E. Stewart: Inst. Phys. Conf. Ser. **125**, 61 (1992)
2. D.M. O'Neill, C.L.S. Lewis, D. Neely, J. Uhomoibhi, M.H. Key, A. MacPhee, G.J. Tallents, S.A. Ramsden, A. Rogowski, A. McLean, G.J. Pert: Opt. Commun. **75**, 406 (1990)
3. D. Neely, C.L.S. Lewis, D.M. O'Neill, J. Uhomoibhi, M.H. Key, G.J. Tallents, S.A. Ramsden: Opt. Commun. **87**, 231 (1992)
4. C.L.S. Lewis, D. Neely, D.M. O'Neill, J. Uhomoibhi, M.H. Key, Y. Al Hadithi, G.J. Tallents, S.A. Ramsden: Opt. Commun. **91**, 71 (1992)
5. A. Carillon, H.Z. Chen, P. Dhez, L. Dwivedi, J. Jacoby, P. Jaeglé, G. Jamelot, Jie Zhang, M.H. Key, A. Kidd, A. Klisnick, R. Kodama, J. Krishnan, C.L.S. Lewis, D. Neely, P. Norreys, D. O'Neill, G.J. Pert, S.A. Ramsden, J.P. Raucourt, G.J. Tallents, J. Uhomoibhi: Phys. Rev. Lett. **68**, 2917 (1992)
6. R.E. Burge: King's College London (private communication)
7. G.J. Pert: York University (private communication)